MDPI

Review

Review of Cell-Balancing Schemes for Electric Vehicle Battery Management Systems

Adnan Ashraf [1], Basit Ali [1], Mothanna S. A. Alsunjury [1,2], Hakime Goren [1], Halise Kilicoglu [1], Faysal Hardan [1] and Pietro Tricoli [1,*]

[1] Department of Electronics, Electrical and Systems Engineering, University of Birmingham, Birmingham B15 2TT, UK; axa1757@student.bham.ac.uk (A.A.); bxa241@student.bham.ac.uk (B.A.); msa954@student.bham.ac.uk or mothanna.sh.aziz@ntu.edu.iq (M.S.A.A.); hxg793@student.bham.ac.uk (H.G.); hxk061@student.bham.ac.uk (H.K.); f.hardan@bham.ac.uk (F.H.)
[2] Technical Engineering College of Mosul, Northern Technical University, Mosul 41001, Iraq
* Correspondence: p.tricoli@bham.ac.uk

Abstract: The battery pack is at the heart of electric vehicles, and lithium-ion cells are preferred because of their high power density, long life, high energy density, and viability for usage in relatively high and low temperatures. Lithium-ion batteries are negatively affected by overvoltage, undervoltage, thermal runaway, and cell voltage imbalance. The minimisation of cell imbalance is particularly important because it causes uneven power dissipation by each cell and, hence, temperature distribution that adversely impacts the battery lifetime. Several papers in the literature proposed advanced cell-balancing techniques to increase the effectiveness of basic cell-balancing approaches, reduce power losses, and reduce the number of components in balancing circuits. The new developments and optimisations over the last few years have been particularly intense due to the increased interest in battery technologies for several end-use applications. This paper reviews and discusses recent cell-balancing techniques or methods, covering their operating principles and the optimised utilisation of electrical components.

Keywords: battery management systems; cell imbalance; electric vehicles; cell balancing; state of charge; active/passive cell balancing

1. Introduction

Globally, battery-powered electric vehicles (EVs) have become a very efficient and practical form of clean transportation. The safety and proper operation of lithium-ion (Li-ion) battery packs, composed of series-connected cells, require an advanced battery management system (BMS) [1]. This system controls every aspect of the battery pack, including temperature [2,3], safety [4,5], charging and discharging, cell voltage and current monitoring [6], fault diagnosis, data acquisition [4], battery state of charge (SOC) and state of health (SOH) [4,7], and cell balancing [8–14]. The latter ensures that all cell voltages are within the desired range, thus optimising usage and lifetime. Cell balancing is one of the most important and challenging parts of the BMS and is based on efficient algorithms to balance either the cell voltages or the SOC.

In fact, it is well known that cell imbalance has a detrimental effect on the performance, safety, and overall lifespan of Li-ion battery systems [15]. When cells are not balanced, some cells may become overcharged, while others remain undercharged. On one hand, overcharged cells can lead to accelerated ageing, reduced capacity, and safety hazards such as thermal runaway and cell failure. On the other hand, undercharged cells reduce the battery pack's overall energy storage capacity, resulting in decreased system performance and reduced reliability [16]. The voltage or SOC imbalance between the cells increases after multiple charge and discharge cycles, progressively damaging the cells and shortening battery service life [17]. Cell imbalance can be caused by a variety of conditions, including

variations in cell capacity, internal resistance, self-discharge rates, and different ageing characteristics. The imbalance may happen during battery production or grow over time because of changes in cell usage and ageing [18,19].

Cell balancing can be carried out through energy dissipation, charge transfer across cells, or cell bypass as discussed in [20,21]. In general, the traditional cell-balancing topologies are classified as passive and active cell balancing, as shown in Figure 1.
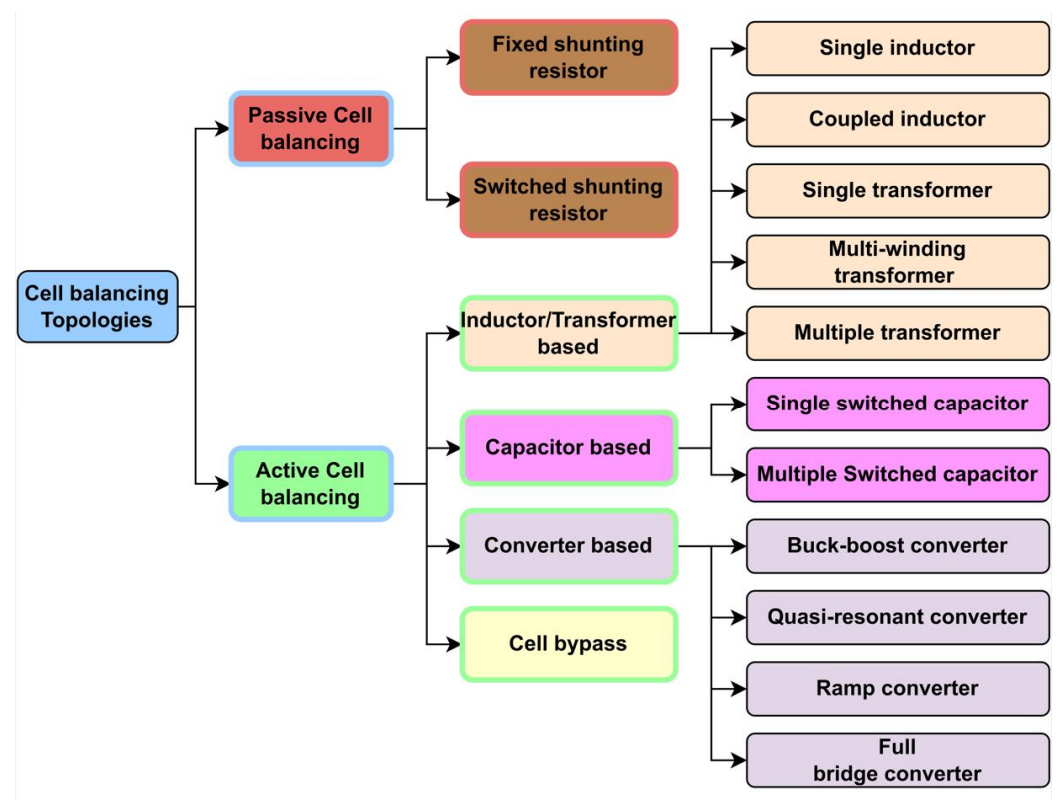
Figure 1. A chart of the basic cell-balancing topologies.

Numerous methods for cell balancing were suggested to increase battery pack efficiency and achieve cell equilibrium. Each method has merits and drawbacks of its own in terms of performance, efficiency, and cost. The advantages and disadvantages of traditional cell-balancing approaches are covered in many review papers in the literature [22–31]; however, these studies do not concentrate on current developments or the optimisation of cell-balancing techniques.

In [22], the authors compared the basic cell-balancing methods focusing on energy storage components and discussed the advantages and limitations of passive and active cell-balancing topologies. Within the context of EVs, Ref. [23] discussed different types of EV technologies and drivetrain architectures, as well as various types of batteries used in EVs. The authors also noted that existing charging equalisation circuits made significant contributions to the safe and efficient operation of EVs, but there are still challenges to overcome to achieve efficient equalisation and enhance battery performance and lifespan. Article [24] examined the general features of Li-ion batteries and made comparisons with alternative battery types. The article also explained the basic cell-balancing techniques and concentrated on the features of BMS. In [25], the effects of variation in temperature and vibration on the cell-balancing performance over an extended period were examined. Article [26] explained the fundamental cell-balancing topologies but with a primary focus on Li-ion battery inconsistencies, which is an important issue to identify and make suitable recommendations for the design of BMSs that are safe, long-lasting, and reasonably cost-effective. Article [27] covered an in-depth examination of EV systems and drivetrain

architectures, as well as the fundamental charge-balancing circuits along with their benefits and drawbacks. This article also discussed a few other EV powertrain architecture-related issues, including raw material and supply chain, driving range efficiency, the need for a sensitive BMS, and the power electronics interface. An overview of the fundamental cell-balancing circuits based on capacitors, inductors, and transformers is presented in [28], which compared all topologies in terms of number of components, cost, circuit volume, control complexity, and balancing current flow. Article [29] described the main features of cell-balancing topologies, including their limitations, and covered the control schemes utilised in battery cell balancers. A detailed examination of active cell balancing using DC/DC converters is covered in [30]. This reference provides comprehensive information about DC/DC converter control principles in addition to SOC estimation, which has an impact on balancing performance. In [31], the authors provided a comprehensive examination of all aspects of BMS, including various battery models, cell-balancing methodologies, BMS issues, and suggestions for solving these issues. Additionally, many factors for modelling the batteries and cell balancers are demonstrated in the paper, including the simulation of eight battery cells connected in series via MATLAB/Simulink software (R2023a) for testing basic active and passive cell-balancing strategies.

In view of the increased demand for Li-ion batteries and EVs in recent years, cell balancing has become a timely topic for scientists, engineers, and scholars. In the past few years, several research publications on new cell-balancing techniques have been released. However, to the author's knowledge, no recent publications provide a comprehensive summary of research studies over the last five years that address the developments and optimisation of cell-balancing techniques. These articles have been searched on Scopus, IEEE, and Google Scholar. The authors technically reviewed and filtered out these articles by finding the articles which provided a clear description of methods, results analysis, data, and balancing control strategies.

This paper is organised in the following manner. Section 2 explains the closed-loop switched-capacitor structure, whilst Section 3 introduces the parallel resonant switched-capacitor equaliser. In Section 4, a description of a single inductor bidirectional active equalisation technique is covered. Section 5 explains the coupled inductor cell-balancing topology, whilst Section 6 presents the structure of a single inductor cell balancing with an auxiliary battery. In Section 7, the double-layer inductive equalisation circuit is explained in detail, while Section 8 illustrates the advanced switched-capacitor equaliser circuit. Section 9 covers the aspects of push–pull converter-based cell-balancing circuits, and Section 10 describes the dual DC-DC converter-based cell-balancing technique with an auxiliary battery. Section 11 reviews the latest articles concerning the single resonant converter balancing circuit, whilst Section 12 provides a summary of optimisation in basic cell-balancing topologies. In Section 13, the conclusions are drawn.
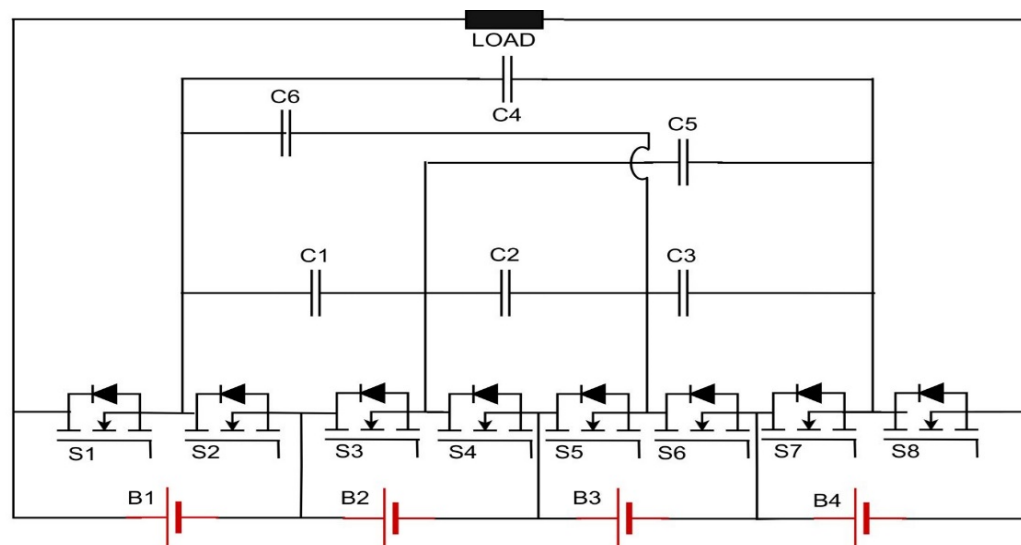
2. Closed-Loop Switched-Capacitor Structure

The switched-capacitor techniques can be classified into two categories. To provide precise balancing paths between cells, the first category includes a large number of switches in chain structures of equalisers with multiple switches and series and parallel equalisers [31,32]. However, the techniques within this category have some drawbacks due to the need for more switches, more voltage stress on the switches, bulkiness, poor dependability, and extra cost. The charging capacitor that connects the balancing circuit structure, like a parallel-structured switched capacitor [33], and the double-tiered switched-capacitor equaliser [34] fall into the second category. This approach reduces the number of switches but has the drawback of decreasing the balancing current, which results in a slower cell-balancing time, and hence the overall battery cell-balancing efficiency can be reduced.

In [35], a cell-balancing technique based on a closed-loop switched-capacitor structure (CLSCS) was developed, utilising PI control to address the above-mentioned problems. Two major contributions are made by the research reported in the paper. Firstly, a CLSCS architecture is used to provide voltage equalisation between any two cells. This structure

is small, less expensive, and highly effective in achieving fast voltage equalisation under any voltage imbalance scenario. Secondly, optimal switching frequencies can be achieved by verifying the battery cell voltage performance under various switching frequency conditions.

The circuit diagram of a proposed CLSCS cell-balancing approach for a battery string with four series-connected cells is shown in Figure 2. The switches (*S1, S2, . . ., S8*) connect the capacitors (*C1, C2, . . ., C6*) to each battery cell (*B1, B2, B3, B4*). Strong balancing, robustness, and ease of modularization are achieved by the symmetrical structure that connects all the capacitors. As compared with the basic double-tiered capacitor cell balancing, this topology adds one extra capacitor to join the first and last cells.

Figure 2. Circuit diagram of the closed-loop switched-capacitor structure, redrawn from [35].

The proposed CLSCS topology was implemented using four Li-ion cells connected in series, and the suggested scheme provided an acceptable performance for cell balancing, as the voltage difference between cells was reduced to less than 0.1 V at the end of the balancing process during the charging stage. Several switching frequencies were used to test the suggested approach. The optimal switching frequency for this circuit was considered to be 28.57 kHz which provided a higher balancing power-efficiency of 95%. The proposed method can be implemented on a high number of cells connected in series; however, in such cases, it will require a greater number of switches and capacitors associated with each cell.
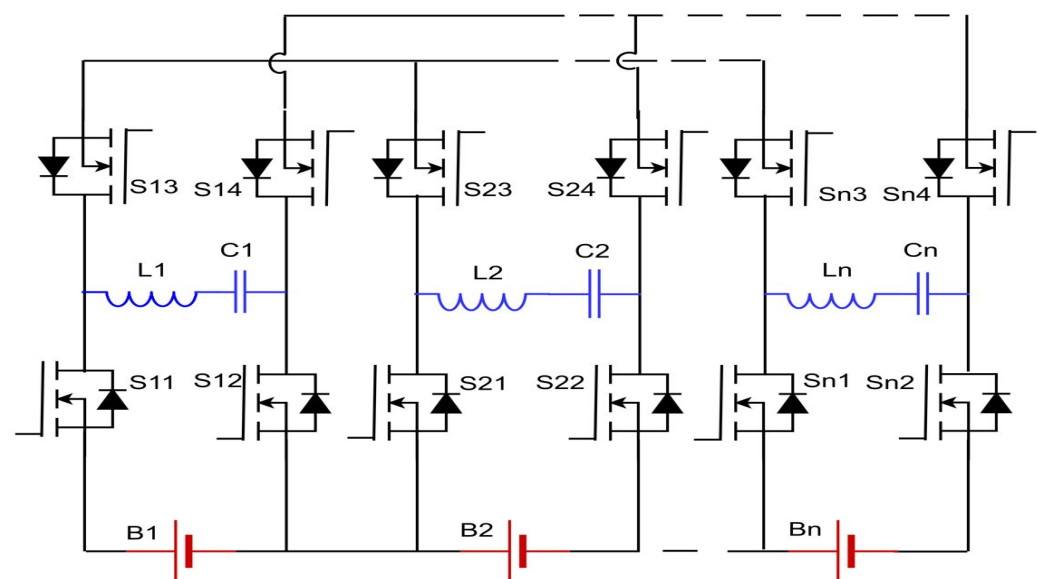
3. Parallel Resonant Switched-Capacitor Equaliser

Recently, resonant switched-capacitor (ReSC) converters have drawn more interest than pure switched-capacitor (PSC) converters because of their higher efficiency [36–39]. The power density of the circuit is improved because the switching frequency can be substantially reduced by approximately the quality factor of the circuit [40,41]. As a result, the ReSC has been used in resonant switched-capacitor equalisers (ReSCE) as proposed in [37]. The advantage of the ReSCE topology is to limit the inrush current flowing through the components by using the LC circuit for energy transfer that operates at a certain resonant frequency. However, the ReSCE can only transfer energy between two adjacent cells. A star-structured circuit using ReSC converters was proposed in [39], which aimed at reducing the inrush current and improving balancing speed, but there is no direct way to transfer energy from the first cell to the last cell.

Resonant switched-capacitor equalisation was proposed in [42], which used ReSC to eliminate the inrush current to achieve minimal output impedance by using the ReSC at a lower switching frequency. The extra energy supplied to the parallel ReSC, was directly

transferred to the low-voltage battery cell. The proposed ReSCE method added an inductor in series with the capacitor to limit the capacitor inrush current that otherwise can be high without the inductor as in the PSC method. The addition of this inductor allows the capacitor to charge to a higher voltage/energy level, permitting more energy transfer between cells while avoiding inrush current issues. This accelerates the balancing speed compared with the PSC topology implemented in [36]. Two complementary PWM signals at fixed frequency were used to control each switch in the system.

Figure 3 illustrates the circuit diagram of the suggested ReSCE for a series-connected battery string. Each battery cell (*B1*) relates to four MOSFETs (*S11*, *S12*, *S13*, *S14*), an inductor (*L1*), and a capacitor (*C1*) to form an ReSC converter, connected in parallel with each battery cell. For the n-th cell, Sn1 and Sn2 create a series connection between the cell and converter, whereas a parallel connection is created by Sn3 and Sn4. The positive pulse of PWM controls Sn1 and Sn2, while the negative pulse controls Sn3 and Sn4.

Figure 3. Circuit diagram of the parallel resonant switched-capacitor equaliser, redrawn from [42].

The findings demonstrated that the proposed ReSCE circuit resulted in a cell-balancing speed three times higher than that of the basic PSC equaliser, in addition to inrush current elimination. However, the ReSCE equaliser generally costs more than the conventional PSC balancers because the PSC uses a single capacitor while ReSCE uses one inductor and a capacitor per cell.

4. Single Inductor Bidirectional Cell Balancing

Conventional balancing circuits with single inductors have recently been improved in several ways, for example, with the cell-to-cell (C2C) balancing approach [43,44], adjacent cell balancing (ACB), cell-to-pack (C2P) balancing [45,46], C2P and pack-to-cell (P2C) balancing [47,48], and pack-to-pack (P2P) balancing. These approaches have the potential to produce suitable equalisation speed, efficiency, and flexibility. However, the increase in circuit size and components adds more complexity to the circuits and their controllers.

A single inductor bidirectional (SIB) cell-balancing technique utilising an inductor with multiple channels for balancing current was proposed in [49], with the objective to achieve fast balancing speed, depending on the switching duty cycle. The proposed balancing circuit provides flexibility in terms of energy transfer modes of operation, as the energy can be transferred from any cell to any cell, cell to pack, and pack to cell. This circuit offers multiple balancing routes for cell balancing; however, the controller complexity will be increased to handle unbalanced states using multiple routes.

Based on the design found in references [50,51], the balancing circuit with low internal resistance bidirectional switches is depicted in Figure 4. To optimise the cell-balancing rate and minimise the balancing time, the different modes of operation, C2C, C2P, and P2C that include multiple balancing paths for balancing current were suggested. The battery pack has *N* cells (*B1*, *B2*, . . ., *Bn*) connected in series; each cell is connected to two bi-directional pairs of switches (e.g., *S1*, *S2*, *S3*, *S4* for *B1*).
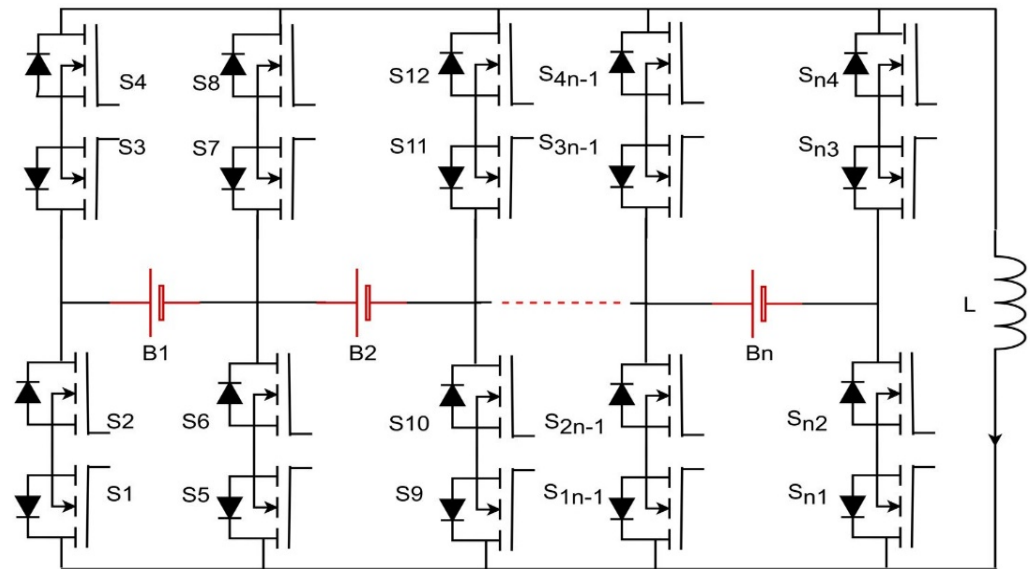
Figure 4. Circuit diagram of single inductor bidirectional cell balancing, redrawn from [49].

The proposed topology was tested for the same initial voltage imbalance of 0.118 V between four connected cells but with different duty cycles (0.6 to 0.85). The results show that the average balancing current went up when the duty cycle increased from 0.6 to 0.75. However, when the duty cycle increased further from 0.75 to 0.85, the average balancing current was reduced. As this current is directly proportional to the balancing speed in this method, faster balancing can be achieved when the duty cycle between 0.6 and 0.75. The effect of the duty cycle on the overall efficiency of the cell balancing was tested, demonstrating that the increase in duty cycle led to a lower power efficiency for the C2C balancing topology.

5. Coupled Inductor Cell Balancing

The idea behind this active cell-balancing method is to transfer energy between cells and a battery pack and to minimise power loss [52,53], as it provides a faster balancing time because of the comparatively high balancing current [54]. However, the method has drawbacks like high cost and magnetic losses, and the high number of circuit components required to achieve greater accuracy of control. The basic inductor-based cell-balancing technique transfers energy throughout the entire pack using a single inductor, whilst, in traditional multi-switched inductor balancing, *N* cells need to be balanced using N − 1 inductors [55].

In [56], the authors proposed a coupled inductor cell-balancing topology that can achieve faster equalisation whilst requiring fewer inductors than the conventional multi-switched inductor balancing approach. The conventional coupled inductor topology requires two inductors while the proposed topology requires one inductor per two cells. Figure 5 shows the circuit diagram of the proposed approach, which consists of four coupled inductors, eight MOSFETs, and eight battery cells (*B1*, *B2*, . . ., *B8*). The mutual inductance of inductor *L1* with other inductors are *M12*, *M13*, and *M14*. The circuit operating principle can be explained in two steps. In step one, the inductors that connect to the cells through one of the switches S1, S3, S5, and S7 transfer and store the energy from high voltage

cells. In the second step, this energy is then distributed to the nearby cells using one of the switches S2, S4, S6, and S8, when they are turned on while the other switches are off. For example, if cell 1 is the high energy/voltage cell in the battery pack, then the energy from cell 1 will be transferred to inductor L1 through switch S1, then this stored energy will be transferred from the inductor to cell 2 through switch S2. The proposed system used the same switching frequency (45.5 kHz in the paper) for all switches with a 45% duty cycle to avoid short circuits. To verify the reliability of the proposed topology, two cases of different initial voltage imbalances (0.8 V and 1.2 V) were considered for experimental testing. The results show zero residual voltage imbalance on average, with a variation band of ± 0.2 V due to noise. The feasibility of the proposed topology was verified using the outcomes of the simulation study and experiments.
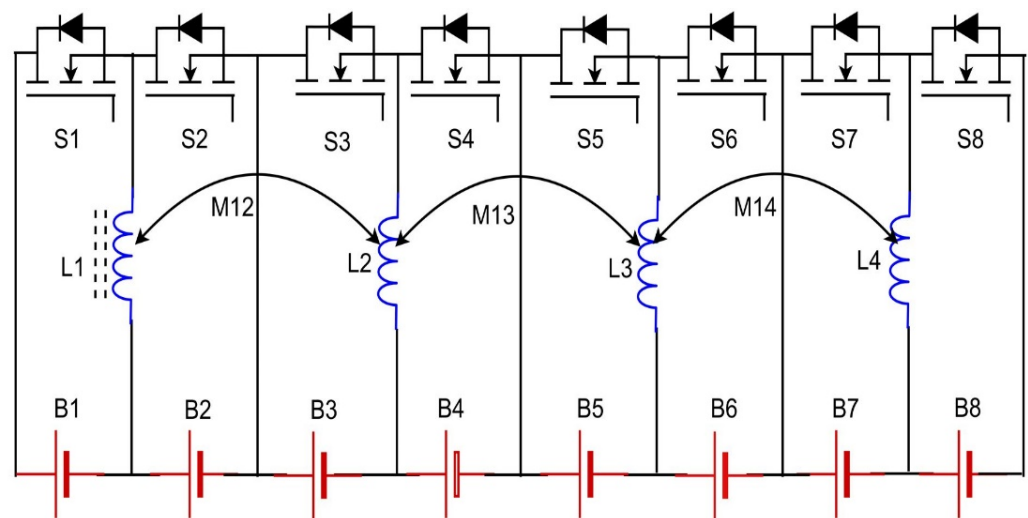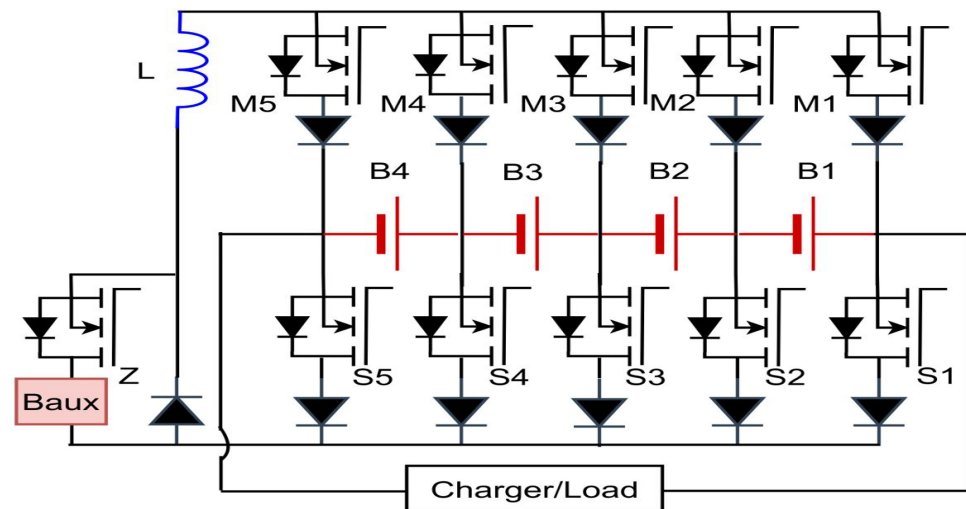

Figure 5. Circuit diagram of coupled inductor cell balancing, redrawn from [56].

6. Single Inductor Cell Balancing with an Auxiliary Battery

This topology was proposed in [53] which is a single inductor cell-balancing circuit utilising an auxiliary battery. The SOC-based control strategy was applied to this topology for cell balancing, which was based on SOC estimation through an adaptive extended Kalman filter. To activate the cell-balancing process during charging, the strategy first calculates the average cell SOC, then compares this SOC with the SOC of each cell considering an SOC threshold. The aim of using the average SOC as a reference was to avoid repeating energy transfer between two lower SOC cells with an SOC difference lower than the threshold.

The circuit diagram of this cell-balancing topology is simple and straightforward, as depicted in Figure 6. The four battery cells (*B1*, *B2*, *B3*, *B4*) are connected in series, whilst the diodes are connected in series with MOSFET switches (*S* and *M*) to prevent short circuits. The auxiliary battery (*Baux*), linked to the inductor (*L*) through a power MOSFET switch (*Z*), forms an inductive energy storage element. The control system then regulates the corresponding power switches and performs cell balancing that transfers energy from the cell to the pack. The energy transfer rate between cells during the cell-balancing process can be controlled by modulating the switch pulses or control signal, whilst the equaliser adjusts the balancing current and hence the balancing rate.

Figure 6. Circuit diagram of a single inductor cell balancing with an auxiliary battery, redrawn from [53].

7. Double-Layer Inductive Equalisation Circuit

The research reported in [57] suggested a double-layer inductive equalisation circuit (DLIEC) to address the balancing of cells, and also implemented the coupled inductor equaliser as presented in [58] to compare the results of cell-balancing time. The DLIEC is depicted in Figure 7. A group of switches (*S11*, *S22*, ..., *Sn1*, *Sn2*) are connected to inductors (*L11*, *L22*, ..., *Ln1*), where switches (*S1*, *S2*, ..., *Sn*) of the balancing submodules are connected to the inductor *L1*. Individual cells within each module can be balanced first when the equalisation circuit is activated, and after that, the modules can be balanced, and the switches are controlled accordingly to obtain the equilibrium state. The control algorithm of this circuit is based on SOC estimation using the particle filter (PF) algorithm. The controller was initialised with random particles that represent the open circuit voltages and SOC relationships, then the mean value of each particle was estimated by updating its weight accordingly to attain the estimated SOC.
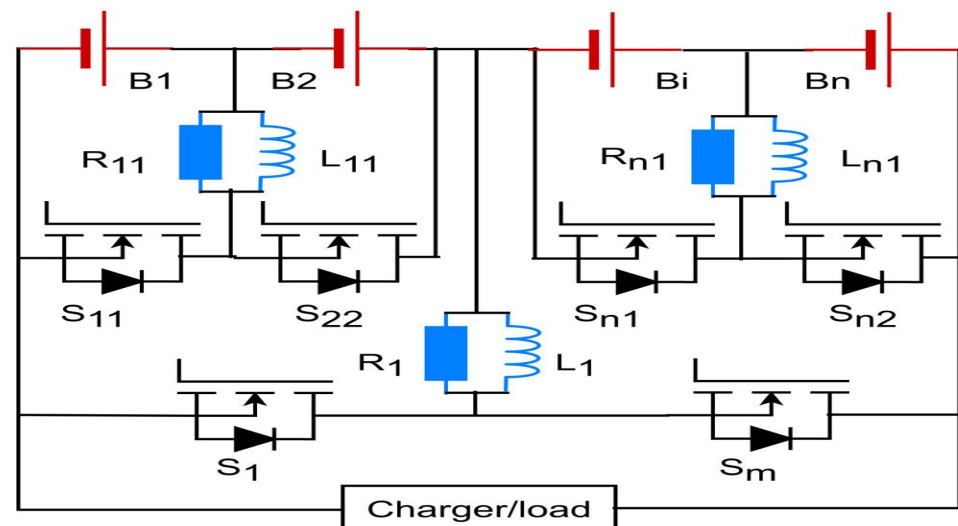
Figure 7. Circuit diagram of the parallel resonant switched-capacitor equaliser, redrawn from [57].

The overall designed system of the DLIEC can firstly be built using a combination of the layering concept and the inductance balancing circuit principle, which can achieve equilibrium within the series-connected cells as well as between the modules of the battery pack. Secondly, the SOC is selected as a control variable for the balancing process, then

the balancing control algorithm can be implemented for the series-connected cells and modules. In this article, eight Li-ion cells were connected in series to perform testing of the cell-balancing process with three modes of operation, charging, discharging, and static mode. According to the reported simulation results, the proposed DLIEC succeeded in fast cell balancing, as compared with those reported in [58] to demonstrate the performance of the proposed topology, particularly in terms of balancing speed. The results showed that the initial maximum SOC imbalance between eight cells was 20%, which reduced to zero residual imbalance in both topologies. However, DLIEC balances the cells in 3172 s, while the coupled inductor topology takes 5001 s for static mode.

8. Advanced Switched-Capacitor Equaliser Circuit

An innovative cell-balancing mechanism for series-connected cells was implemented and reported in [59] by integrating Cuk and buck-boost converters. Its main goal was to minimise the number of switches and management of the balancing circuit by two complementary switching signals at a 50% duty cycle. Typically, the buck-boost or the Cuk converter needs (2N − 1) switches while the proposed topology combines the two converters and requires only N switches for N battery cells. However, this balancing mechanism has three shortcomings:

1. At the switching instances, the capacitor charging and discharging currents are extremely high.
2. The voltage of the cells does not change significantly throughout one or more switching cycles. Here, if a fixed duty cycle of 50% is used with cells having different voltages and linked to a single inductor through the switches, the inductor volt-second balance law will not be satisfied, leading to a rise in the average inductor current.
3. The balancing speed will drastically decrease if the number of series cells increases due to the utilisation of traditional switched-capacitor (SC)-based topology, which can only offer adjacent cell balancing.

The authors of [60] have provided an advanced cell-balancing circuit that combines series LC converters and buck-boost converters in an attempt to find a solution for the first shortcoming, but this article does not address the other two problems. However, in [61], an advanced switched-capacitor equaliser circuit (ASCEC) was proposed, considering the effects of parasitic resistance (*RC* and *RL*) of capacitor (*C*) and inductor (*L*) and the principle of SC and a buck-boost cell-balancing system, to resolve the above shortcomings 2 and 3. The proposed balancing topology is composed of two tiers: the first tier is formed by the SC topology while the second tier is generated from the buck-boost topology, which was used to equalize the submodules connected in series.

In Figure 8, cells (*Bn1* and *Bn2*) are connected in series to create a module and these modules (*B1*, *B2*, . . ., *Bn*) are further connected in series to make up a battery pack. The common switch array between the two tiers has the same number of switching transistors as the battery cells. This balancing topology uses the same number of capacitors and inductors, which are equal to the number of modules. A simple control algorithm is used to control the switches to connect or disconnect the cells with the balancing structure, using complementary PWM switching signals to control the switching transistors.

Considering the influence of parasitic resistance of the magnetic components, the cell-balancing topology based on the SC and buck-boost converter cell balancer was implemented in this proposed circuit. The parasitic resistance adversely affected the balancing speed; thus, the value of this resistance must be decreased to reduce the balancing time. According to the simulation and experimental findings, the proposed cell-balancing method effectively addressed the issue of voltage imbalance for series-connected battery cells and the imbalance was reduced to 18 mV from 132 mV. When compared with earlier converter-based topologies, this method significantly requires fewer switches and achieves fast balancing, as only two complementary PWM signals are needed to operate the entire system.
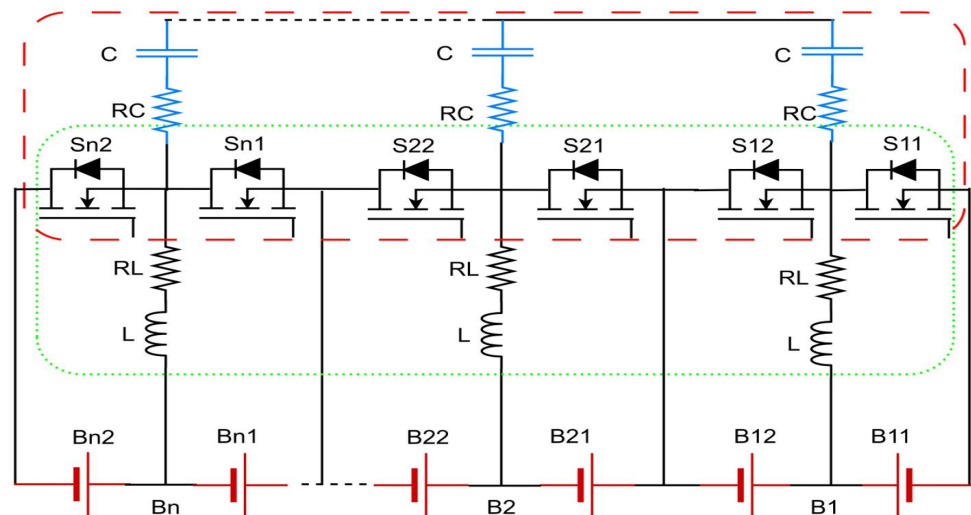
Figure 8. Circuit diagram of the advanced switched-capacitor equaliser circuit, redrawn from [61].

9. Push-Pull Converter-Based Cell-Balancing Circuit

In article [62], a push-pull converter was introduced to transfer the energy between cells using relays instead of using MOSFETs to reduce the cost while adopting simple control implementation. The control strategy of the suggested method is straightforward and simple for implementation. The voltage gain of the push-pull converter needs to be adjusted precisely to maintain the balancing current when the voltage difference becomes smaller, and thus fast cell balancing can be achieved.

In [62], the suggested C2C balancing topology consists of three primary blocks, as depicted in Figure 9. The switching network is the first block that connects each battery cell to each converter terminal so that charge can be transferred. The second block consists of the push-pull converter and is used to transfer the charge from the strong cell to the weak cell. The digital signal processor (DSP) and a monitoring integrated circuit (IC) are the third block, which controls the operation of the converter's power switches and regularly updates the information of each cell voltage.
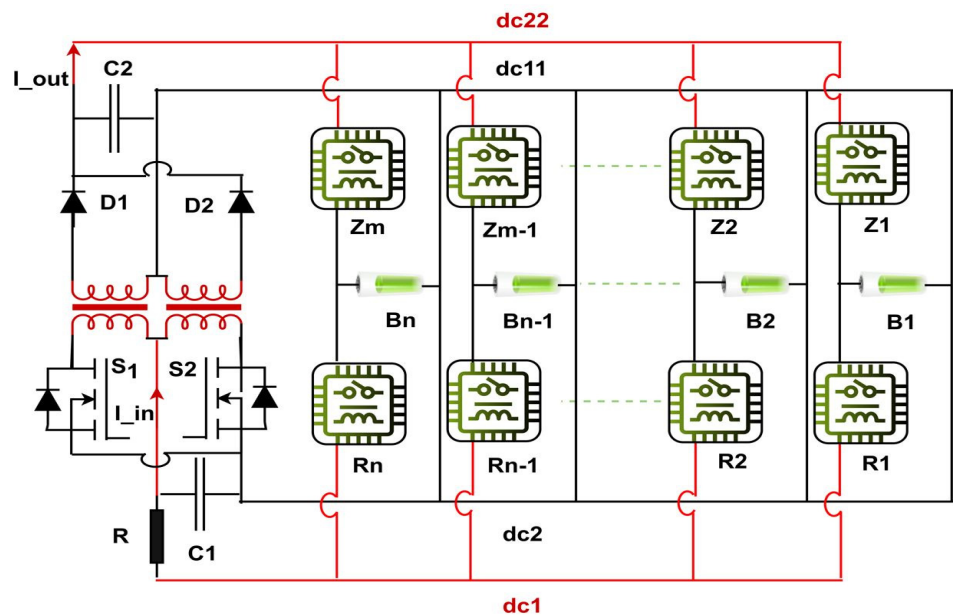

Figure 9. Circuit diagram of push-pull converter-based cell balancing, redrawn from [62].

There are two strings of relays in the switching network: the converter primary side which is connected to one side of the battery cells through the DC buses (*dc1* and *dc2*) via a single chain of relays (*R1*, *R2*, . . ., *Rn*), and the converter secondary side which is connected to the other side of the battery cells via the DC buses (*dc11* and *dc22* through another chain of relays (*Z1*, *Z2*, . . ., *Zm*). The proposed topology can transfer charge from any cell to any other cell within the battery pack. The switching transistors are used as driving circuitries for connection to the relays, which can help in lowering the cost of the balancing topology when compared to other topologies that use MOSFETS. To lower the cost of the entire system further, the IC and controller may utilise the same power source.

The simple design, controllability, and high efficiency of the isolated push-pull converter make the converter a preferred choice for balancing. The transformer's turns ratio can be set to 1:1 if the converter's parts are in ideal condition. However, the voltage drops of these parts must be considered while designing the converter to increase the voltage. To compensate for the voltage drops, the transformer structure shown in Figure 9 was designed with a 1:1.2 turns ratio. The duty cycle of the converter switches was also set to 50% to provide minimal voltage and current ripples during the charging or discharging of the Li-ion cells.

The IC of voltage measurement checks each cell voltage and sends the values to a digital signal processor (DSP) via a serial I^2C communication link, whilst the measurement of the balancing current can be taken using a current-sensing resistor on the primary side of the transformer.

The experimental findings demonstrate that the suggested method performed exceptionally well in terms of balancing time, taking only 50 min to finish the balancing of 12 cells while charging was taking place. In the proposed topology, the cells shift energy directly from high-voltage cells to low-voltage cells.
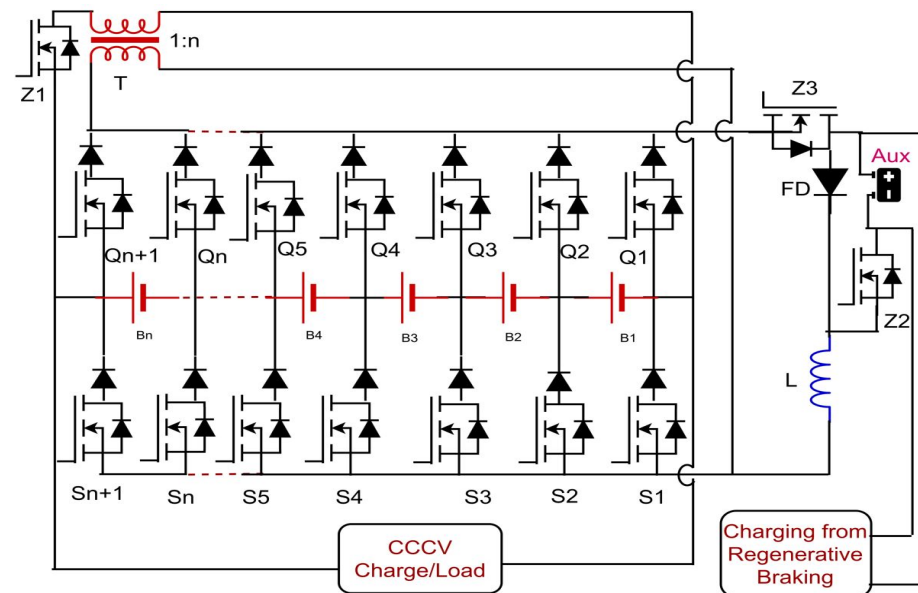
10. Dual DC-DC Converter-Based Cell Balancing with an Auxiliary Battery

The structure of the dual DC-DC converter-based cell balancing with an auxiliary battery is reported in [63]. This topology is based on both voltage and SOC-based control algorithms which are more efficient due to the precise control for selecting the high-voltage cells, albeit SOC estimation requires a complex control algorithm. As such, it eliminates P2C energy transfer during the process of cell balancing, and further, the architecture allows the energy produced by the regenerative braking to be utilised for charging the auxiliary battery, which will make the balancing efficiency even better.

Figure 10 depicts the circuit structure of the proposed DC-DC converter-based cell balancing topology. The proposed circuit contains, 2n + 2 MOSFET power switches and diodes, one transformer (*T*), one inductor (*L*), and a freewheeling diode (*FD*) connected to an auxiliary battery. The constant current constant voltage (CCCV) charger and load are connected to the terminals of the battery pack, which is accordingly used for charging and discharging processes. Since the inductor is used for C2P balancing, a transformer with a turns ratio of 1: n is necessary. This strategy was proposed to offer C2P balance during charging whilst utilising an auxiliary battery during discharging. The inductor and affiliated MOSFET switches (*Z2* and *Z3*) construct a flyback converter while the auxiliary battery is connected to the inductor through the MOSFET switches (*Z1* and *Z2*) to create a buck converter. The flyback converter here is responsible for C2P balancing during charging, while the buck converter is used to charge the auxiliary battery from the regenerative braking recovered during discharging. The balancing speed of the switch can be regulated by adjusting its pulse width modulated (PWM) signal, which can also control the balancing current.

The suggested system employed a traditional buck-converter cell-balancing technique during the discharging phase and a flyback converter cell-balancing technique during the charging phase. When a series of simulation tests was performed using four Li-ion cells using the Matlab/Simulink software, the cell-balancing system demonstrated the difference between the SOC/voltage-based control methods. The connected Li-ion cells were tested

with a maximum 20% SOC and 0.11 V voltage difference. The imbalance was reduced to 1% SOC and 0.01 V voltage at the end of the charging or discharging process. However, it was noticed that the balancing time for the SOC based controller was 1984 s, while for the voltage-based controller, it was 2486 s for the same initial imbalance. Although the SOC-based control gives a faster balancing speed, the correct SOC estimate is difficult to obtain and, therefore, voltage-based equalisation approaches are preferred in practice.

Figure 10. Circuit diagram of a dual DC-DC converter-based cell balancing with an auxiliary battery, redrawn from [63].

11. Single Resonant Converter Balancing Circuit

In article [64], a single resonant converter active balancing circuit is proposed, shown in Figure 11. The paper mainly reports on an active balancing circuit, which is based on a single resonant converter, where the energy transfer method improves cell-to-cell (C2C) balancing. The proposed topology optimises the balancing circuit presented in [65] by reducing the number of switches from 4N to $4(N - 1)$. The switching and resonant frequency become equal to attain soft switching to reduce switching loss, where all switches are controlled in near zero current switching (ZCS).
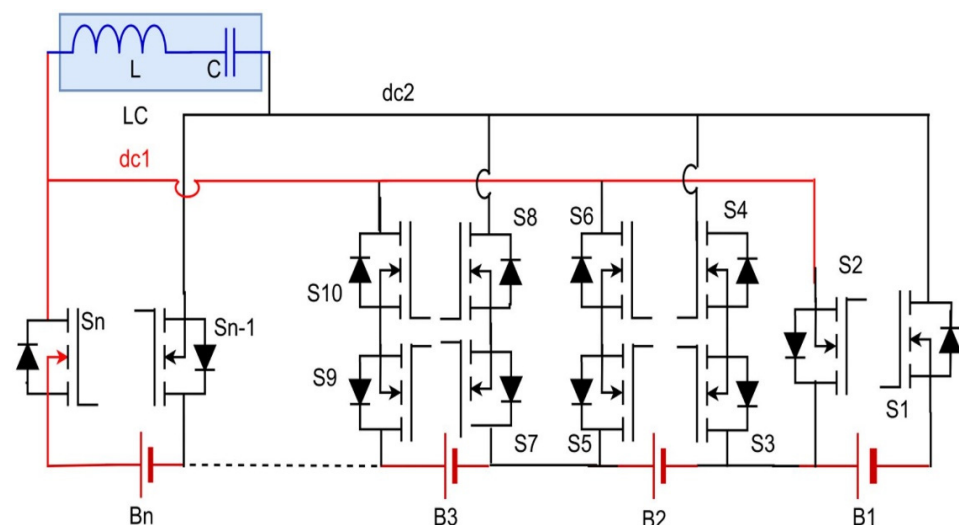
Figure 11. Circuit diagram of single resonant converter balancing, redrawn from [64].

The purpose of the resonant tank is to store the energy from the strong battery cell, which is connected to both sides of individual battery cells through a bus wire (*dc1* and *dc2*) and MOSFET switches (*S1, S2, ..., Sn*), as shown in Figure 11. The energy transfer process is carried out in two stages; in the first half cycle, the energy is stored in the resonant tank from the strong cell, and in the next half cycle, the stored energy is transferred to the weak cell from the resonant tank. A cell monitoring IC is provided for each cell to sense the voltages of all cells connected in series and transfer the data to the microcontroller to perform the cell-balancing procedure. Complementary PWM signals are used to turn the MOSFET switches On or OFF throughout the balancing process, thus the proposed circuit requires simpler digital control. In the article, a simulation study was performed using the MATLAB Simulink program to confirm the theoretical analysis and to analyse the results before hardware implementation. The simulation results of two battery cells showed zero residual imbalance at the end of the cell-balancing process. The switching frequency used in this circuit was the same as the switching frequency of the resonant tank.

12. Summary of Optimisation in Basic Cell-Balancing Topologies

Recent advancements and optimisation in cell-balancing techniques are summarised and presented in Table 1. Their circuit topologies and optimised results have also been remarked. Determining the preferred techniques by comparison based on the available information, results, and data could not be performed with proper accuracy. All techniques reported in the literature were tested under different initial conditions, cell parameters, and even using switches at different power levels. However, in terms of cells' residual imbalance voltage, the reported methods in [56,57,64] demonstrated 0 V residual voltages, or zero SOC at the end of the balancing process. Also, the methods documented in [61,62] approximately produced the same results. If the number of switching devices/relays is considered to increase the total cost of the balancing topology, then the methods reported in [56,61] are the ones which only employ one switch per cell.

In terms of cell-balancing speed, a comparison between the reported methods was not visible, as all available data were measured/evaluated with different levels of initial imbalance. However, the authors elicited an indicative balancing time by dividing the cell capacity in *Ah* by its balancing current used at each balancing method, as shown in Table 1. Physically, this time represents the time needed to balance a difference in energy capacity between cells equivalent to the cell capacity, as applied for all methods based on the available data. In this context, the method reported in [61] seems to have delivered the shortest indicative time of 0.52 h. Nevertheless, the performance for all methods, in terms of balancing speed, can always be enhanced by increasing the level of balancing currents or sharing power between the cells of the battery pack.

Table 1. Recent advancements and optimisations of cell-balancing techniques.

Ref.	Type	Reported Technique	Initial Imbalance (%)	Residual Imbalance (%)	Capacity of Li-Ion Cell (Ah)	Balancing Current (A)	Indicative Cell-Balancing Speed (Hour)	No. of Switches	Control Method	Remarks
[35]	Switched capacitor	Closed loop switched-capacitor equaliser	34.86% voltage	2.97% voltage	2.6	1.72	1.51	2N	SOC based	The experimental results only show the final residual difference between cells but can explain cell balancing. One extra capacitor was added, for joining the first and last cell.
[42]	Switched capacitor	Parallel resonant switched-capacitor equaliser	8.1% voltage	0.01% voltage	1.1	0.4	2.75	4N	Voltage based	**It gives a three times higher cell-balancing speed than the basic PSC equaliser by reducing inrush current**.
[49]	Inductor based	Single inductor bidirectional cell balancing	6.3% voltage	0.5% voltage	20	0.8	25	4N + 4	Voltage based	**Achieved fast balancing speed by using optimal switching duty cycle and providing multiple balancing paths**. However, continuous increase in duty cycle can reduce the balancing time and lead to lower efficiency.
[56]	Inductor based	Coupled inductor cell balancing	24.24% voltage	**Approx. zero**	n/a	2	n/a	**N**	Voltage based	Used simulation for static balancing and experiment for charge balancing, but they used inductor voltage to prove cell balancing instead of battery cell—that is why the cell balancing took only 6 s. **The number of switches compared with traditional coupled inductor topology is reduced by one switch per cell pair.**
[53]	Inductor based	Single inductor cell balancing with an auxiliary battery	30.2% SOC	**0% SOC**	12.8	6.4	2	2N + 3	SOC based	The average SOC was selected as a control variable to activate cell-balancing process. Use of an auxiliary battery to accept energy from high-voltage cells and transfer it to low-voltage cells.
[57]	Inductor based	Double-layer inductive equalisation circuit with a resistor in parallel with each inductor	25% SOC	**0% SOC**	n/a	7	n/a	N + N/2	SOC based	The proposed system used dual-layer inductor topology and **compared the results with a single layer inductor to provide better performance of the proposed system**. Also tested at 0.5C, 1C and 2C rates, but the paper does not show the charging results, so illustrating identical results during both charging and discharging.

Table 1. *Cont.*

Ref.	Type	Reported Technique	Initial Imbalance (%)	Residual Imbalance (%)	Capacity of Li-Ion Cell (Ah)	Balancing Current (A)	Indicative Cell-Balancing Speed (Hour)	No. of Switches	Control Method	Remarks
[61]	Capacitor and inductor based	Advanced switched-capacitor equaliser circuit	19.86% voltage	**Approx. zero**	2	3.82	**0.52**	**N**	Voltage based	By considering the influence of parasitic resistance of the magnetic components, this cell-balancing topology was based on the switched capacitor, and a buck-boost converter for implementation.
[62]	Converter based	Push-pull converter-based cell-balancing circuit	6.75% voltage	**Approx. zero**	n/a	1.5	n/a	4 switches, 2N relays	Voltage based	It used an isolated push-pull converter to directly transfer energy from one cell to another for balancing. **The duty cycle of the converter switches is set to 50% to provide minimal voltage and current ripples**.
[63]	Converter based	Dual DC-DC converter-based cell balancing with an auxiliary battery	20% SOC	1% SOC	n/a	4	n/a	2N + 5	SOC and voltage based	The inductor and affiliated switches build a flyback converter, while an auxiliary battery connected with the inductor through switches creates a buck converter, known as dual DC-DC converter-based cell-balancing topology. The flyback converter is responsible for C2P balancing during charging, while **the buck converter is used to charge the auxiliary battery from regenerative braking during discharging**.
[64]	Resonant converter	Single resonant converter balancing circuit with reduced resonant frequency	5.4% voltage	**Approx. zero**	4.2	1	4.2	4(N − 1)	Voltage based	**A single resonant converter with reduced resonant frequency is used to improve balancing time and reduce power losses as compared with independent resonant tank topology**. The proposed topology is also tested for supercapacitor and lead-acid battery cell balancing, other than lithium-ion battery cells.

N: number of battery's cells, n/a: not available.

13. Conclusions

The main objective of this article is to review recent trends in cell-balancing methods for lithium-ion batteries. An in-depth study was undertaken to explain the operating principles and control algorithms of the cell-balancing methods published most recently in the literature. The review concluded that recent cell-balancing topologies are based mostly on inductors, capacitors, and a combination of both. Generally, the efficiency and cell-balancing speed are increased by adding a few extra inductors or capacitors to the basic cell-balancing topologies. However, adding more inductors or capacitors requires extra semiconductor switches, which slightly increase the power losses of balancing circuits. Some balancing topologies use an auxiliary battery to supply or draw energy during the cell-balancing process. Furthermore, DC-DC converters have also gained attention in recent years for cell-balancing circuits. Resonant converters have been used to reduce switching losses, as they operate near zero voltage/current switching. Other topologies, like buck-boost, push-pull, and Cuk converters are used in balancing circuits to stabilise the battery output voltage and decrease cell-balancing time. However, the size, volume and weight of the balancing circuits will increase when adopting such converters.

References

1. Lee, S.B.; Thiagarajan, R.S.; Subramanian, V.R.; Onori, S. Advanced Battery Management Systems: Modeling and Numerical Simulation for Control. In Proceedings of the 2022 American Control Conference (ACC), Atlanta, GE, USA, 8–10 June 2022; pp. 4403–4414.
2. Altemose, G.; Hellermann, P.; Mazz, T. Active cell balancing system using an isolated share bus for Li-Ion battery management: Focusing on satellite applications. In Proceedings of the 2011 IEEE Long Island Systems, Applications and Technology Conference, Farmingdale, NY, USA, 6 May 2011; pp. 1–7.
3. Hu, L.; Zhao, M.-L.; Wu, X.-B.; Lou, J.-N. Cell balancing management for battery pack. In Proceedings of the 2010 10th IEEE International Conference on Solid-State and Integrated Circuit Technology, Shanghai, China, 1–4 November 2010; pp. 339–341.
4. Gabbar, H.A.; Othman, A.M.; Abdussami, M.R. Review of battery management systems (BMS) development and industrial standards. *Technologies* **2021**, *9*, 28. [CrossRef]
5. Cadar, D.V.; Petreus, D.M.; Patarau, T.M. An energy converter method for battery cell balancing. In Proceedings of the 33rd International Spring Seminar on Electronics Technology, ISSE 2010, Warsaw, Poland, 12–16 May 2010; pp. 290–293.
6. Shen, M.; Gao, Q. A review on battery management system from the modeling efforts to its multiapplication and integration. *Int. J. Energy Res.* **2019**, *43*, 5042–5075. [CrossRef]
7. Wen, S. Cell balancing buys extra run time and battery life. *Analog Appl. J.* **2009**, *1*, 14–41.
8. Liu, K.; Li, K.; Peng, Q.; Zhang, C. A brief review on key technologies in the battery management system of electric vehicles. *Front. Mech. Eng.* **2019**, *14*, 47–64. [CrossRef]
9. Wang, Y.; Tian, J.; Sun, Z.; Wang, L.; Xu, R.; Li, M.; Chen, Z. A comprehensive review of battery modeling and state estimation approaches for advanced battery management systems. *Renew. Sustain. Energy Rev.* **2020**, *131*, 110015. [CrossRef]
10. Lü, X.; Wu, Y.; Lian, J.; Zhang, Y.; Chen, C.; Wang, P.; Meng, L. Energy management of hybrid electric vehicles: A review of energy optimization of fuel cell hybrid power system based on genetic algorithm. *Energy Convers. Manag.* **2020**, *205*, 112474. [CrossRef]
11. Wu, B.; Widanage, W.D.; Yang, S.; Liu, X. Battery digital twins: Perspectives on the fusion of models, data and artificial intelligence for smart battery management systems. *Energy AI* **2020**, *1*, 100016. [CrossRef]
12. Dai, H.; Jiang, B.; Hu, X.; Lin, X.; Wei, X.; Pecht, M. Advanced battery management strategies for a sustainable energy future: Multilayer design concepts and research trends. *Renew. Sustain. Energy Rev.* **2021**, *138*, 110480. [CrossRef]
13. İnci, M.; Büyük, M.; Demir, M.H.; İlbey, G. A review and research on fuel cell electric vehicles: Topologies, power electronic converters, energy management methods, technical challenges, marketing and future aspects. *Renew. Sustain. Energy Rev.* **2021**, *137*, 110648. [CrossRef]

14. Ali, M.U.; Zafar, A.; Nengroo, S.H.; Hussain, S.; Junaid Alvi, M.; Kim, H.-J. Towards a smarter battery management system for electric vehicle applications: A critical review of lithium-ion battery state of charge estimation. *Energies* **2019**, *12*, 446. [CrossRef]

15. Hemavathi, S. Overview of cell balancing methods for Li-ion battery technology. *Energy Storage* **2021**, *3*, e203.

16. Thiruvonasundari, D.; Deepa, K. Optimized passive cell balancing for fast charging in electric vehicle. *IETE J. Res.* **2023**, *69*, 2089–2097. [CrossRef]

17. Quraan, M.; Tricoli, P.; D'Arco, S.; Piegari, L. Efficiency assessment of modular multilevel converters for battery electric vehicles. *IEEE Trans. Power Electron.* **2016**, *32*, 2041–2051. [CrossRef]

18. Hoekstra, F.S.J.; Ribelles, L.W.; Bergveld, H.J.; Donkers, M. Real-time range maximisation of electric vehicles through active cell balancing using model-predictive control. In Proceedings of the 2020 American Control Conference (ACC), Denver, CO, USA, 1–3 July 2020; pp. 2219–2224.

19. Zhang, D.-H.; Zhu, G.-R.; He, S.-J.; Qiu, S.; Ma, Y.; Wu, Q.-M.; Chen, W. Balancing control strategy for li-ion batteries string based on dynamic balanced point. *Energies* **2015**, *8*, 1830–1847. [CrossRef]

20. Hasan, M.K.; Mahmud, M.; Habib, A.A.; Motakabber, S.; Islam, S. Review of electric vehicle energy storage and management system: Standards, issues, and challenges. *J. Energy Storage* **2021**, *41*, 102940. [CrossRef]

21. Borne, M.; Wen, S. Providing Active Cell Balancing in Battery Design. Texas Instruments. EE Times-India. Lehtiartikkeli. Saatavissa. 2009. Available online: http://eetindia.com (accessed on 3 January 2024).

22. Lee, Y.; Jeon, S.; Lee, H.; Bae, S. Comparison on cell balancing methods for energy storage applications. *Indian J. Sci. Technol.* **2016**, *9*, 92316. [CrossRef]

23. Hoque, M.; Hannan, M.; Mohamed, A.; Ayob, A. Battery charge equalization controller in electric vehicle applications: A review. *Renew. Sustain. Energy Rev.* **2017**, *75*, 1363–1385. [CrossRef]

24. Vaideeswaran, V.; Bhuvanesh, S.; Devasena, M. Battery management systems for electric vehicles using lithium ion batteries. In Proceedings of the 2019 Innovations in Power and Advanced Computing Technologies (i-PACT), Vellore, India, 22–23 March 2019; Volume 1, pp. 1–9.

25. Omariba, Z.B.; Zhang, L.; Sun, D. Review of battery cell balancing methodologies for optimizing battery pack performance in electric vehicles. *IEEE Access* **2019**, *7*, 129335–129352. [CrossRef]

26. Hua, Y.; Zhou, S.; Cui, H.; Liu, X.; Zhang, C.; Xu, X.; Ling, H.; Yang, S. A comprehensive review on inconsistency and equalization technology of lithium-ion battery for electric vehicles. *Int. J. Energy Res.* **2020**, *44*, 11059–11087. [CrossRef]

27. Habib, A.A.; Hasan, M.K.; Mahmud, M.; Motakabber, S.; Ibrahimya, M.I.; Islam, S. A review: Energy storage system and balancing circuits for electric vehicle application. *IET Power Electron.* **2021**, *14*, 1–13. [CrossRef]

28. Carter, J.; Fan, Z.; Cao, J. Cell equalisation circuits: A review. *J. Power Sources* **2020**, *448*, 227489. [CrossRef]

29. Das, U.K.; Shrivastava, P.; Tey, K.S.; Idris, M.Y.I.B.; Mekhilef, S.; Jamei, E.; Seyedmahmoudian, M.; Stojcevski, A. Advancement of lithium-ion battery cells voltage equalization techniques: A review. *Renew. Sustain. Energy Rev.* **2020**, *134*, 110227. [CrossRef]

30. Turksoy, A.; Teke, A.; Alkaya, A. A comprehensive overview of the dc-dc converter-based battery charge balancing methods in electric vehicles. *Renew. Sustain. Energy Rev.* **2020**, *133*, 110274. [CrossRef]

31. Uzair, M.; Abbas, G.; Hosain, S. Characteristics of battery management systems of electric vehicles with consideration of the active and passive cell balancing process. *World Electr. Veh. J.* **2021**, *12*, 120. [CrossRef]

32. Anno, T.; Koizumi, H. Double-input bidirectional DC/DC converter using cell-voltage equalizer with flyback transformer. *IEEE Trans. Power Electron.* **2014**, *30*, 2923–2934. [CrossRef]

33. Ye, Y.; Cheng, K.W.E.; Fong, Y.C.; Xue, X.; Lin, J. Topology, modeling, and design of switched-capacitor-based cell balancing systems and their balancing exploration. *IEEE Trans. Power Electron.* **2016**, *32*, 4444–4454. [CrossRef]

34. Fukui, R.; Koizumi, H. Double-tiered switched capacitor battery charge equalizer with chain structure. In Proceedings of the IECON 2013-39th Annual Conference of the IEEE Industrial Electronics Society, Vienna, Austria, 10–13 November 2013; pp. 6715–6720.

35. Singirikonda, S.; Obulesu, Y. Active cell voltage balancing of Electric vehicle batteries by using an optimized switched capacitor strategy. *J. Energy Storage* **2021**, *38*, 102521. [CrossRef]

36. Ye, Y.; Cheng, K.W.E. Modeling and analysis of series–parallel switched-capacitor voltage equalizer for battery/supercapacitor strings. *IEEE J. Emerg. Sel. Top. Power Electron.* **2015**, *3*, 977–983. [CrossRef]

37. Yuanmao, Y.; Cheng, K.W.E.; Yeung, Y. Zero-current switching switched-capacitor zero-voltage-gap automatic equalization system for series battery string. *IEEE Trans. Power Electron.* **2011**, *27*, 3234–3242. [CrossRef]

38. Lee, K.-M.; Chung, Y.-C.; Sung, C.-H.; Kang, B. Active cell balancing of li-ion batteries using LC series resonant circuit. *IEEE Trans. Ind. Electron.* **2015**, *62*, 5491–5501. [CrossRef]

39. Ye, Y.; Cheng, K.W.E. Analysis and design of zero-current switching switched-capacitor cell balancing circuit for series-connected battery/supercapacitor. *IEEE Trans. Veh. Technol.* **2017**, *67*, 948–955. [CrossRef]

40. Pasternak, S.R.; Kiani, M.H.; Rentmeister, J.S.; Stauth, J.T. Modeling and performance limits of switched-capacitor DC–DC converters capable of resonant operation with a single inductor. *IEEE J. Emerg. Sel. Top. Power Electron.* **2017**, *5*, 1746–1760. [CrossRef]

41. Kesarwani, K.; Sangwan, R.; Stauth, J.T. Resonant-switched capacitor converters for chip-scale power delivery: Design and implementation. *IEEE Trans. Power Electron.* **2014**, *30*, 6966–6977. [CrossRef]

42. Liu, L.; Mai, R.; Xu, B.; Sun, W.; Zhou, W.; He, Z. Design of parallel resonant switched-capacitor equalizer for series-connected battery strings. *IEEE Trans. Power Electron.* **2021**, *36*, 9160–9169. [CrossRef]

43. Shang, Y.; Zhang, C.; Cui, N.; Mi, C.C. A delta-structured switched-capacitor equalizer for series-connected battery strings. *IEEE Trans. Power Electron.* **2018**, *34*, 452–461. [CrossRef]

44. Shang, Y.; Xia, B.; Zhang, C.; Cui, N.; Yang, J.; Mi, C.C. An automatic equalizer based on forward–flyback converter for series-connected battery strings. *IEEE Trans. Ind. Electron.* **2017**, *64*, 5380–5391. [CrossRef]

45. Du, W.; Huang, X.; Yang, S.; Zhang, F.; Wu, X.; Qian, Z. A novel equalization method with defective-battery-replacing for series-connected lithium battery strings. In Proceedings of the 2009 IEEE Energy Conversion Congress and Exposition, San Jose, CA, USA, 20–24 September 2009; pp. 1806–1811.

46. Mestrallet, F.; Kerachev, L.; Crebier, J.-C.; Collet, A. Multiphase interleaved converter for lithium battery active balancing. *IEEE Trans. Power Electron.* **2013**, *29*, 2874–2881. [CrossRef]

47. Wang, Y.; Zhang, C.; Chen, Z.; Xie, J.; Zhang, X. A novel active equalization method for lithium-ion batteries in electric vehicles. *Appl. Energy* **2015**, *145*, 36–42. [CrossRef]

48. Wei, J.; Dong, G.; Chen, Z.; Kang, Y. System state estimation and optimal energy control framework for multicell lithium-ion battery system. *Appl. Energy* **2017**, *187*, 37–49. [CrossRef]

49. Chen, Y.; Liu, X.; Shen, T.; Cheng, L.; Wang, X.; Yang, R.; Yang, S. An any-cell (s)-to-cell (s) equalization method with a single magnetic component for Lithium-ion battery pack. *J. Energy Storage* **2021**, *33*, 102071. [CrossRef]

50. Park, S.-H.; Kim, T.-S.; Park, J.-S.; Moon, G.-W.; Yoon, M.-J. A new battery equalizer based on buck-boost topology. In Proceedings of the 2007 7th Internatonal Conference on Power Electronics, Daegu, Republic of Korea, 22–26 October 2007; pp. 962–965.

51. Yarlagadda, S.; Hartley, T.T.; Husain, I. A battery management system using an active charge equalization technique based on a DC/DC converter topology. *IEEE Trans. Ind. Appl.* **2013**, *49*, 2720–2729. [CrossRef]

52. Imtiaz, A.M.; Khan, F.H.; Kamath, H. A low-cost time shared cell balancing technique for future lithium-ion battery storage system featuring regenerative energy distribution. In Proceedings of the 2011 Twenty-Sixth Annual IEEE Applied Power Electronics Conference and Exposition (APEC), Fort Worth, TX, USA, 6–11 March 2011; pp. 792–799.

53. Zhang, Z.; Zhang, L.; Hu, L.; Huang, C. Active cell balancing of lithium-ion battery pack based on average state of charge. *Int. J. Energy Res.* **2020**, *44*, 2535–2548. [CrossRef]

54. Moghaddam, A.F.; Van Den Bossche, A. An active cell equalization technique for lithium ion batteries based on inductor balancing. In Proceedings of the 2018 9th International Conference on Mechanical and Aerospace Engineering (ICMAE), Budapest, Hungary, 10–13 July 2018; pp. 274–278.

55. Moghaddam, A.F.; Van den Bossche, A. Multi-winding equalization technique for lithium ion batteries for electrical vehicles. In Proceedings of the 2018 7th International Conference on Renewable Energy Research and Applications (ICRERA), Paris, France, 14–17 October 2018; pp. 139–143.

56. Farzan Moghaddam, A.; Van den Bossche, A. An efficient equalizing method for lithium-ion batteries based on coupled inductor balancing. *Electronics* **2019**, *8*, 136. [CrossRef]

57. Liu, X.; Pang, H.; Geng, Y. Dual-Layer Inductor Active Equalization Control for Series-Connected Lithium-Ion Batteries Based on SOC Estimation. *Electronics* **2022**, *11*, 1169. [CrossRef]

58. Ma, Y.; Duan, P.; Sun, Y.; Chen, H. Equalization of lithium-ion battery pack based on fuzzy logic control in electric vehicle. *IEEE Trans. Ind. Electron.* **2018**, *65*, 6762–6771. [CrossRef]

59. Lu, X.; Qian, W.; Peng, F.Z. Modularized buck-boost+ Cuk converter for high voltage series connected battery cells. In Proceedings of the 2012 Twenty-Seventh Annual IEEE Applied Power Electronics Conference and Exposition (APEC), Orlando, FL, USA, 5–9 February 2012; pp. 2272–2278.

60. Ji, W.; Lu, X.; Ji, Y.; Tang, Y.; Ran, F.; Peng, F.Z. Low cost battery equalizer using buck-boost and series LC converter with synchronous phase-shift control. In Proceedings of the 2013 Twenty-Eighth Annual IEEE Applied Power Electronics Conference and Exposition (APEC), Long Beach, CA, USA, 17–21 March 2013; pp. 1152–1157.

61. Ye, Y.; Lin, J.; Li, Z.; Wang, X. Double-tiered cell balancing system with switched-capacitor and switched-inductor. *IEEE Access* **2019**, *7*, 183356–183364. [CrossRef]

62. Pham, V.-L.; Duong, V.-T.; Choi, W. A low cost and fast cell-to-cell balancing circuit for lithium-Ion battery strings. *Electronics* **2020**, *9*, 248. [CrossRef]

63. Samanta, A.; Chowdhuri, S. Active cell balancing of lithium-ion battery pack using dual DC-DC converter and auxiliary lead-acid battery. *J. Energy Storage* **2021**, *33*, 102109. [CrossRef]

64. Habib, A.A.; Hasan, M.K. Lithium-ion battery state-of-charge balancing circuit using single resonant converter for electric vehicle applications. *J. Energy Storage* **2023**, *61*, 106727. [CrossRef]

65. Yu, Y.; Saasaa, R.; Khan, A.A.; Eberle, W. A series resonant energy storage cell voltage balancing circuit. *IEEE J. Emerg. Sel. Top. Power Electron.* **2019**, *8*, 3151–3161. [CrossRef]